Available online at www.sciencedirect.com
ScienceDirect
Thermochimica Acta 460 (2007) 28–34
thermochimica acta
www.elsevier.com/locate/tca

Dynamic thermogravimetric degradation of gamma radiolytically synthesized Ag–PVA nanocomposites

A.N. Krklješ, M.T. Marinović-Cincović, Z.M. Kačarević-Popović *, J.M. Nedeljković

Vinča Institute of Nuclear Sciences, Mike Petrovića Alasa 12-14, 11001 Belgrade, Serbia

Received 20 November 2006; received in revised form 4 May 2007; accepted 9 May 2007
Available online 21 May 2007

Abstract

The degradation kinetics of gamma radiolytically synthesized Ag–PVA nanocomposites was investigated by thermogravimetric method under dynamic conditions (30–600 °C) in an inert atmosphere. Thermogravimetric analysis showed that thermal degradation of composites was a two-stage process for the lower amount of nanofiller and single-stage for the higher amount of nanofiller. The Vyazovkin model-free kinetics method was applied to calculate the activation energy (E_a) of the degradation process as a function of conversion and temperature. At a given degradation temperature, PVA as a host in nanocomposite presents lower reaction velocity, while its E_a is higher than that of pure PVA.

Keywords: Ag–PVA nanocomposites; Gamma irradiation; Dynamic thermogravimetric analysis; Model-free kinetics

1. Introduction

Much attention has been devoted to the preparation of metal nanoparticles because of their unique properties. Noble metal particles such as silver and gold are of great significance due to their size-dependent optical properties [1–3]. Moreover, size effect was observed for the antibacterial activity of silver nanoparticles [4].

A large number of synthetic procedures have been employed in order to synthesize silver nanoparticles and/or nanocomposites [5–10]. It has been shown that the morphology, particle size distribution, stability and properties of silver nanoparticles as well as the corresponding nanocomposites are strongly dependent on the method of preparation and specific experimental conditions. The radiolytic method is suitable for generating metal particles, particularly silver, in solution [11–16]. The radiolytically generated species, solvated electrons and secondary radicals exhibit strong reduction potentials, and consequently metal ions are reduced at each encounter. The control of particle size is commonly achieved by the use of capping agents such as polymers, which are present in the solution during the formation of metal clusters. Polymer molecules interact with the growing metal particles, inhibiting the aggregation process. In addition, casting of film becomes easier and the particle size can be well controlled within the desired regime. On the other hand, the homogeneous dispersions of nanoparticles more or less lead to a noticeable increase in the degradation temperature of some polymer host, while being harmful to some other polymers [17–21]. The improved thermal stability may be attributed to a barrier model which suggests that a polymeric-inorganic char builds up on the surface of the polymer melt and therefore provides a mass and heat transfer barrier [22]. According to other investigation in several metal-polymer nanocomposites, retardation of thermal degradation was mainly due to suppression of the mobility of polymer chains by the nanoparticles, while accelerating of the degradation was mainly attributed to a decrease in the degradation activation energy due to catalytic role of metal nanoparticles [23]. Metal colloid catalysts are very effective in many-electron processes because they present unusual electron "basins" where the electrons can easily move or escape from. However, the mechanism of such effects is not yet well understood. In particular, the kinetics of the thermal degradation remains unknown.

With the aim of providing a fundamental understanding of the degradation mechanism and the effect of the presence of Ag nanofiller on the thermal stability and degradation of the PVA matrix in an Ag–PVA nanocomposite system, the thermal degradation kinetics was studied. PVA has been used in this work as

* Corresponding author. Tel.: +381 11 2453 986; fax: +381 11 3440 100.
E-mail address: zkacar@vin.bg.ac.yu (Z.M. Kačarević-Popović).

0040-6031/$ – see front matter © 2007 Elsevier B.V. All rights reserved.
doi:10.1016/j.tca.2007.05.015

a matrix for preparation of nanocomposites due to its easy processability, high optical clarity [24] and biocompatibility [25]. The model-free kinetics method proposed by Vyazovkin for determining the kinetic parameters of chemical reactions has been applied to determine the thermal degradation process in many polymers and has given good results [26,27]; however, not much work concerning the determination of the activation energy could be found in the literature to enable estimation of the thermal stability of hybrid nanocomposites. In this study the kinetics of the thermodegradation process in the radiolytically synthesized Ag–PVA nanocomposite was investigated by the model-free kinetics method, in order to define the activation energy required for the degradation process as well as the influence of nanoparticle loading on the thermal stability of this hybrid system.

2. Experimental

2.1. Materials

All chemicals were of analytical grade and used as received. Water was obtained from a Millipore Milli-Q system. $AgNO_3$, 2-propanol and PVA having a molecular weight of 72,000 g mol^{-1} and a degree of hydrolysis of min. 99%, were products of MERK. Ar and N_2 gases were of high purity (99.5%).

2.2. Synthesis of Ag–PVA nanocomposites

The polymer (1.4 mass%) was completely dissolved in boiling water. Solutions containing PVA (1.4 mass%), appropriate concentration of $AgNO_3$ and 2-propanol (0.2 M) were bubbled with argon in order to remove oxygen. Gamma irradiation was performed in a ^{60}Co radiation facility at room temperature up to integral radiation doses of 0.27, 0.53, 1.08, 2.86, 5.64, 9.32 and 12.04 kGy in order to reduce 0.17, 0.34, 0.67, 1.71, 3.51 and 5.79 mM of Ag^+ ions, respectively. The dose rate was approximately 12 kGy/h. Nanocomposite films with contents of inorganic phase in the concentration range from 0.2 to 10 mass% were obtained after the solvent evaporation.

2.3. Characterization of Ag–PVA nanocomposites

The content of Ag in Ag–PVA nanocomposites was determined by Inductively Coupled Plasma-Atomic Emission Spectrometry (ICP-AES), a Perkin-Elmer model ICP/6500. The contents of inorganic phase in the nanocomposite films were found to be 0.20, 0.40, 1.0, 2.5, 5.0, 8.0 and 10.0 mass%.

Transmission electron microscopy (TEM) measurement was done on a Philips EM 400 microscope operated at 120 kV. Thin film was prepared by dropping aqueous dispersion of the nanocomposite on a carbon-coated Cu grid.

Absorption spectra of the Ag–PVA nanocomposite films were recorded using a Perkin-Elmer Lambda 5 spectrophotometer.

The degradation kinetics was measured as temperature dependent mass loss by using a Perkin-Elmer TGS-2 instrument. Polymer samples of 5 mg were placed in a platinum sample holder and heated from ambient temperature to 600 °C at heating rates of 5, 10 and 20 °C min^{-1} in dynamic nitrogen (30 ml min^{-1}). The buoyancy effect in TGA was accounted for by performing empty pan runs and subtracting the resulting data from the subsequent mass loss data.

3. Results and discussion

3.1. Dynamic thermal degradation of Ag–PVA nanocomposites

The advantage of gamma irradiation method in the synthesis of metallic nanoparticles lies in the fact that desired highly reducing radicals can be generated without formation of any byproduct. The primary radicals and molecules produced in water upon gamma irradiation are e_{aq}^- (2.7), $OH^\bullet$ (2.7), $H^\bullet$ (0.6), H_2 (0.45) and H_2O_2 (0.7). The numbers in parentheses represent the respective G values, i.e. number of species formed per 100 eV of absorbed energy. The $OH^\bullet$ and $H^\bullet$ radicals are capable of abstracting hydrogen from the alcohol, producing an alcohol radical [11]. In that way, oxidizing $OH^\bullet$ radicals are transformed into reducing alcohol radicals. In this study, 2-propanol was used to scavenge $OH^\bullet$ radicals. Under the stated experimental conditions the reduction of Ag^+ ions takes place by electron transfer from hydrated electrons and 2-propanol radicals.

Typical absorption spectra of Ag–PVA nanocomposite film, TEM image and size distribution of Ag nanoparticles are shown in Fig. 1. The average size of Ag nanospheres was found to be 6.1 nm, estimated from the histogram. The particle size distribution is broad (the size range is from 3 to 12 nm).

In order to investigate changes in the thermal stability of the PVA arisen from the presence of nanoparticles in the polymer matrix, the thermal properties of the composite were explored. Fig. 2 shows the thermogravimetric (TG) curves of dynamic thermal degradation of pure PVA and Ag–PVA nanocomposites, normalized only to the PVA content (m_{PVA} (%) = ((m_{compos} (%) − m_{Ag} (%))/100 − m_{Ag} (%))×100) obtained in a temperature range of 30–600 °C at heating rates of 5, 10, and 20 °C min^{-1}.

It is evident that the thermal degradation of pure PVA proceeds by two degradation steps, and with the addition of nanofiller the thermal degradation of PVA (highly loaded with Ag nanoparticles) proceeds by a one-step degradation process between 200 and 300 °C (Fig. 2). Moreover, transient char from the thermal decomposition of pure PVA depends on the heating rate, suggesting degradation via competitive reactions. In general, in competitive reactions low temperature is favorable for the reaction with lower activation energy, and the opposite—high temperature is favorable for the reaction with the higher activation energy, which means that slow heating rate is favorable for the reaction with lower activation energy and *vice versa* [28]. The fundamental condensed phase processes which lead to char formation during the thermal degradation of PVA are the chain-stripping elimination of H_2O and the chain-scission reactions which occur in parallel [29].

The main decomposition products in the first step of thermal degradation of pure PVA are polyenes generated from the chain-stripping elimination reaction of H_2O, as well as *cis* and

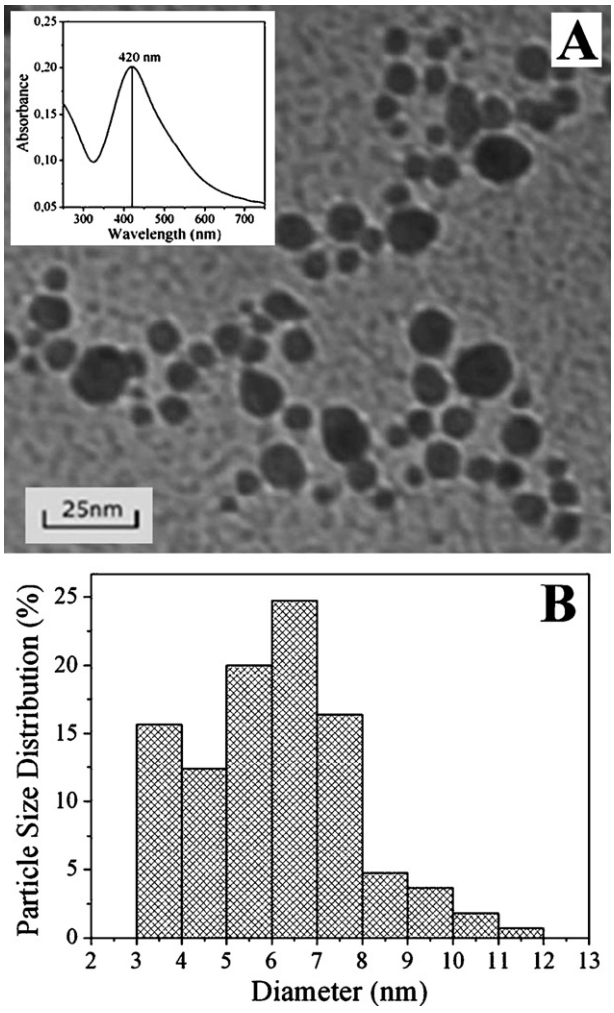

Fig. 1. The TEM micrograph (A), UV–vis absorption spectra (inset in A) and particle size distribution (B) of Ag nanoparticles formed in PVA (0.5% Ag).

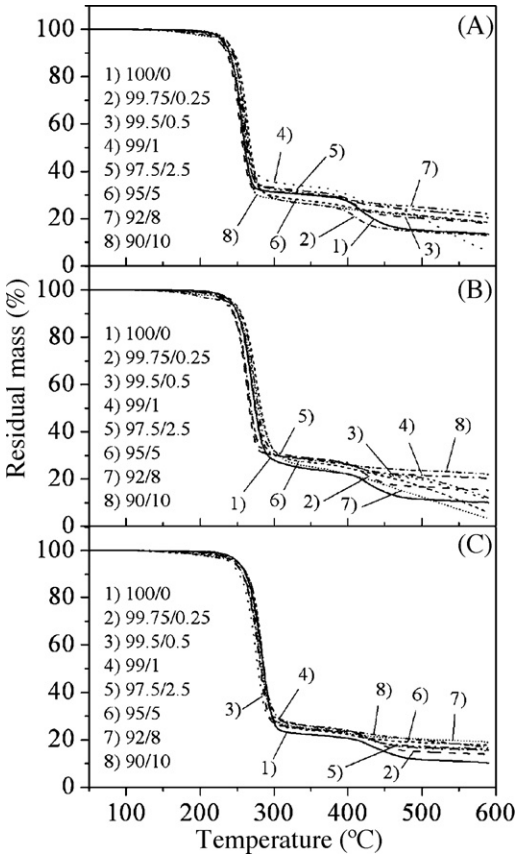

Fig. 2. Normalized TG curves of dynamic thermal degradation of pure PVA and PVA in Ag–PVA nanocomposites at different heating rates: (A) 5 °C min^{-1}; (B) 10 °C min^{-1}; (C) 20 °C min^{-1}.

trans allylic-methyls that may form via random chain scission reactions that accompany elimination. Random chain scission reactions are the reactions that have higher activation energy owing to a rather high C–C bond energy (around 350 kJ mol^{-1}) [26]. These reactions seem to occur preferably during thermal degradation with higher heating rate. They probably have a lower transient char compared to chain-stripping elimination of H_2O. In the second degradation step cyclization (Diels-Alder intramolecular and intermolecular cyclization followed by dehydrogenation with aromatization) and radical reaction pathways, which occur in parallel, are responsible for the conversion of unsaturated carbons into substituted aromatic or aliphatic carbons.

Two general mechanisms are probably responsible for the modes of action of Ag nanoparticles on the thermal degradation of PVA. One is described as a chemical constraint for the H_2O elimination in the first degradation step due to the interaction of Ag nanoparticles with OH groups, which may increase energy barrier of the chain-stripping elimination reaction of H_2O and induce a shift of the thermal degradation of partial decomposition products toward chain scission and formation of methyl terminated polyenes. Indeed, the interaction of OH groups with Ag nanoparticles is confirmed by previous FTIR analysis [11,15]. In addition, Ag nanoparticles may act as radical scavenger suppressing radical transfer to the adjacent chains via intermolecular and intramolecular chain reactions. The other mechanism is described as a physical constraint (reduced molecular mobility) for the reactions of inter and intra cyclization of polyenes in the second degradation step that seem to occur preferably at a lower heating rate compared with radical reaction pathways. Moreover, the decrease in the mobility of the polymer chains may decrease their collision frequency and suppress chain transfer reactions.

Changes in the thermal degradation of PVA are the consequence of the presence of the nanoparticles only, because gamma irradiation (in applied dose range) under the stated experimental conditions does not induce any change in the polymer [30,31].

The characteristics of the TG and differential TG curves: the onset temperatures of degradation (T_1^0) (the intersections of the extrapolated base lines with tangents drawn at the inflection points of the TG curve); the temperatures at the maximum rate of degradation in the first degradation step (T_1^m), obtained from differential curves and the mass losses at the end of the first degradation step, were obtained by applying the Perkin-Elmer Standard program for TGS-2.

The dependencies of onset temperatures (T_1^0) and of the temperatures at the maximum rate of degradation in the first

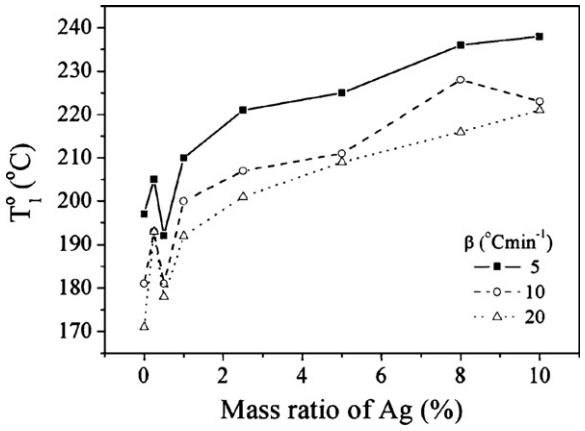

Fig. 3. The effect of PVA/Ag composition and heating rates on the onset temperatures.

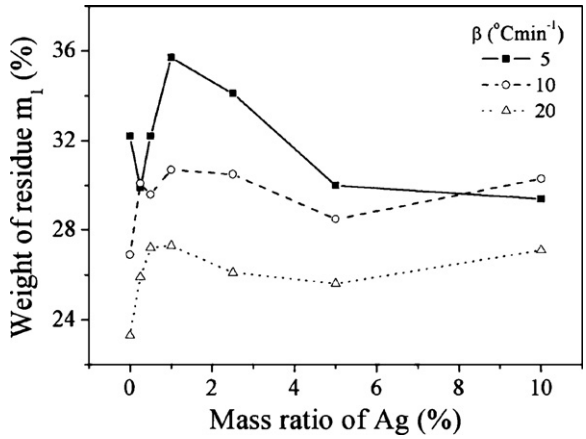

Fig. 5. The effect of PVA/Ag composition and heating rates on the Δm_1.

degradation step (T_1^m) on Ag content in nanocomposites, for different heating rates, are shown in Figs. 3 and 4, respectively.

It is obvious that these characteristics depend on the content of nanofiller. With the addition of Ag nanoparticles, temperatures (T_1^0) are shifted toward higher values. The shift in the beginning of the thermal degradation of PVA to higher values is probably a consequence of the adsorption of polymer on nanoparticles surfaces via OH groups (as measured by FTIR spectrophotometry [11,15]). Hence, in the nanocomposite highly loaded with Ag nanoparticles the anchoring frequency increases (although probably a large fraction of active surface sites remain available) increasing the strength of adsorption energy.

Furthermore, the dependence of the weight of residue at the end of the first degradation step (Δm_1) on the Ag content in nanocomposite for different heating rates is shown in Fig. 5. It can be seen that this degradation stage is completed at a weight of the PVA residue in nanocomposite 6% greater than that of pure PVA. This increase is especially pronounced for the low loading of nanofiller and low heating rate, which means that a smaller number of PVA molecules are degraded at this step. It seems that the greater chain confinement due to better interaction with small amount of Ag nanoparticles suppress degradation via radical reaction pathways and chain transfer reactions. As a consequence, for low loading of nanofiller thermal degradation occur at the lower T_1^m, and have the greater weight of residue, Figs. 4 and 5, respectively. In addition, it was found that at relatively low nanofiller content the introduction of nanofiller increases the crystallinity of PVA, as the nanoparticles could act as heterogeneous nucleating agent during the crystallization [22]. The PVA crystallization is mainly caused by the strong intermolecular hydrogen bonding interaction among the PVA molecular chains. When greater nanofiller content is introduced, the interactions between Ag and PVA illustrated in our previous work with FTIR investigation [11,15] lead to a decrease in the intensity of the intermolecular interaction. Thus, Ag nanoparticles act as a barrier to restrict the formation of crystal. However, the increase in crystallinity occurs at a small amount of nanofiller [32]. The greater crystallinity (stronger hydrogen bonding between the polymer chains via OH groups and lower chain mobility) at relatively low loading of nanofiller in nanocomposite and low heating rate probably could additionally influence the thermal degradation of polymer. Moreover, according to previous investigation [33] other properties of PVA depending on the content of nanofiller are also changed for the low nanofiller loading.

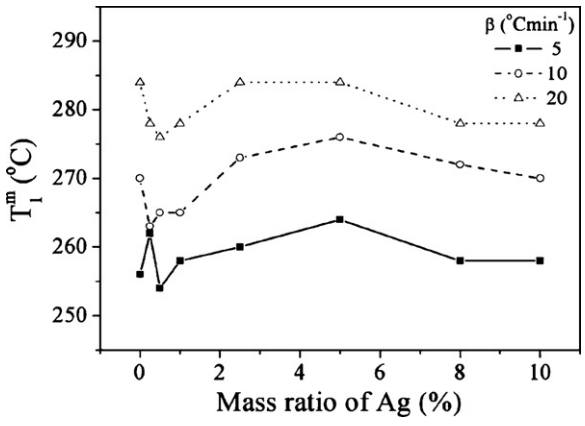

Fig. 4. The effect of PVA/Ag composition and heating rates on the temperatures at the maximum rates of degradation.

3.2. Kinetic analysis

The reaction rate of the thermal and catalytic reaction depends on conversion (α), temperature (T) and time (t). For each process, the reaction rate as a function of conversion, $f(\alpha)$, is different and must be determined from experimental data. Applying the model-free kinetics method, accurate evaluation of complexes reactions can be performed. The model-free kinetics is based on calculation of the effective activation energy (E_a) as a function of the conversion (α) of a chemical reaction $E = f(\alpha)$. A chemical reaction is measured at at least three different heating rates (β) and the respective conversion curves are calculated out of the TG measured curves. For each conversion (α) $\ln \beta/T^2$ is plotted versus $1/T_\alpha$ giving rise to a straight line with slope $-E_{a_\alpha}/R$, therefore providing the activation energy as a function of conversion [34–36].

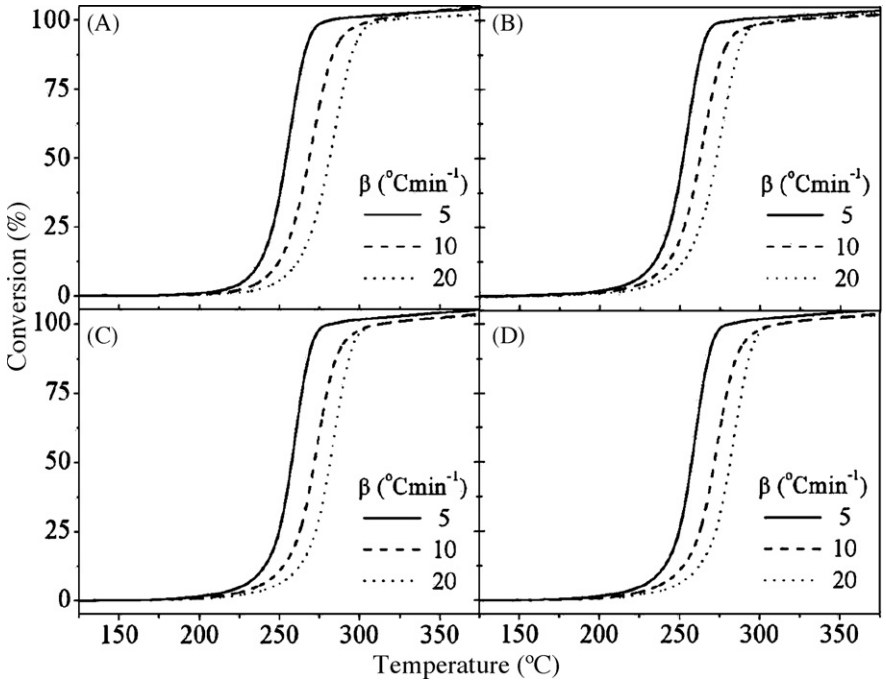

Fig. 6. Conversion of PVA in Ag–PVA nanocomposite: pure PVA (A); 0.5% Ag (B); 2.5% Ag (C); 10% Ag (D), as a function of temperature.

Eq. (1) is defined as a dynamic equation [27], which is used for the determination of the activation energy (E_a) for all conversion values (α):

$$\ln\frac{\beta}{T_\alpha^2} = \ln\left[\frac{Rk_0}{E_{a_\alpha} g(\alpha)}\right] - \frac{E_{a_\alpha}}{R}\frac{1}{T_\alpha} \quad (1)$$

A temperature range of 100–380 °C for the pronounced mass loss in the first degradation step was selected for kinetic studies by means of model-free. Fig. 6 shows the degree of conversion as a function of temperature relative to degradation of pure PVA and PVA in nanocomposite system with 0.5, 2.5 and 10% of Ag nanoparticles. The observation made from curves in Fig. 6 is more evident when examining the plots of degree of conversion versus time, as it is shown in Fig. 7 that was obtained from the model-free data. These graphs show comparative curves between pure PVA and PVA in nanocomposite system at five sets of temperatures: 200, 225, 250, 275 and 300 °C.

One can see clearly that the time for the degradation of pure PVA and PVA in nanocomposite decreases considerably as a function of temperature. At 200 and 225 °C pure PVA degrades faster than PVA in nanocomposite for all composi-

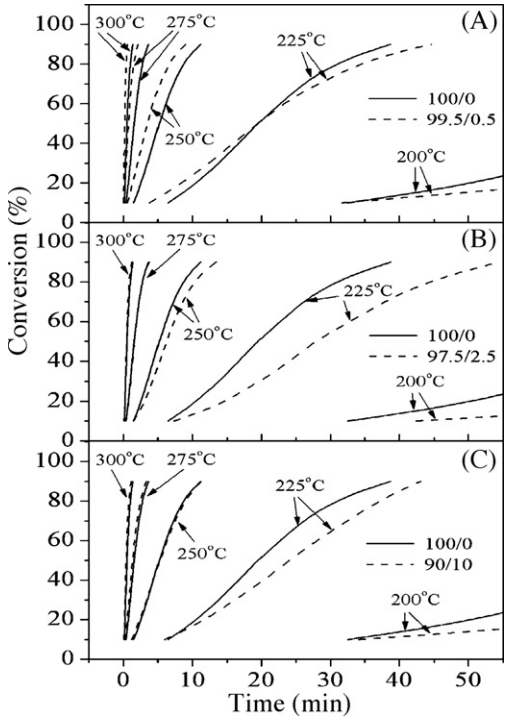

Fig. 7. Conversion of PVA in Ag–PVA nanocomposite (A) 0.5% Ag; (B) 2.5% Ag; (C) 10% Ag, as a function of time, compared with the pure PVA.

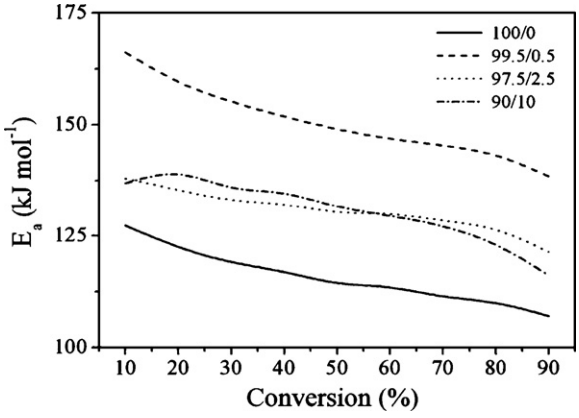

Fig. 8. Dependence of activation energy on conversion (α) for pure PVA and PVA in 0.5, 2.5 and 10% Ag nanocomposites.

Table 1
Isoconversion parameters for pure PVA

Time (min)	Conversion (%)								
	10	20	30	40	50	60	70	80	90
10	491.0	499.0	503.8	507.4	510.5	513.6	516.7	520.4	525.7
30	474.3	481.1	485.0	488.0	490.5	493.2	495.7	498.8	503.1
50	466.9	473.2	476.8	479.5	481.8	484.2	486.5	489.4	493.3
70	462.2	468.2	471.5	474.1	476.1	478.5	480.6	483.4	487.0
90	458.7	464.5	467.6	470.1	472.0	474.3	476.3	479.0	482.4
120	454.8	460.3	463.3	465.6	467.4	469.6	471.5	474.0	477.3

Table 2
Isoconversion parameters for PVA in 0.5% Ag–PVA nanocomposite

Time (min)	Conversion (%)								
	10	20	30	40	50	60	70	80	90
10	486.4	495.9	501.0	504.6	507.6	510.3	513.4	516.7	521.5
30	473.8	482.2	486.7	489.7	492.3	494.6	497.3	500.2	504.2
50	468.1	476.1	480.3	483.1	485.4	487.7	490.2	492.9	496.5
70	464.4	472.2	476.1	478.8	481.1	483.2	485.6	488.2	491.5
90	461.8	469.3	473.1	475.7	477.8	479.9	482.3	484.7	487.9
120	458.7	466.0	469.7	472.1	474.2	476.2	478.5	480.8	483.8

Table 3
Isoconversion parameters for PVA in 2.5% Ag–PVA nanocomposite

Time (min)	Conversion (%)								
	10	20	30	40	50	60	70	80	90
10	493.5	504.0	508.8	512.3	515.0	517.8	520.5	523.8	528.8
30	477.9	487.4	491.7	494.7	497.0	499.6	502.0	504.7	508.5
50	471.0	480.0	484.1	487.0	489.1	491.6	493.8	496.3	499.6
70	466.5	475.3	479.2	482.0	484.0	486.4	488.5	490.9	494.0
90	463.2	471.9	475.6	478.4	480.3	482.6	484.7	486.9	489.8
120	459.5	468.0	471.6	474.2	476.1	478.4	480.3	482.5	485.1

tions. At 250 °C the same is observed for the 2.5% Ag loading, but not for the 0.5% Ag loading. For the higher temperatures of degradation, PVA as a host in nanocomposite degrades faster than pure PVA. At 300 °C, PVA practically degrades in a few minutes, both pure and in the nanocomposite system.

The activation energy (E_a) for the thermal degradation process of PVA and the PVA in nanocomposite, predicted by the model-free kinetics theory, is shown in Fig. 8. The standard deviation was in the range from 0.02 with Ag loading of 0.5% to 0.1 with Ag loading of 2.5%. Note that the activation energy for pure PVA is lower than that for the degradation of PVA in nanocomposite. At a given degree of conversion (E_a) of PVA in nanocomposite is for 20 kJ mol^{-1} greater than that of pure PVA. This difference is even more pronounced with an Ag loading of 0.5%. This means that Ag nanofiller increases the energy barrier of the thermal degradation process even in the very small amount. This remarkable effect of influence of such a small amount of the Ag nanoparticles on the thermal stability of the PVA matrix was already observed for Ag–PVA nanocomposites obtained by chemical reduction method [33].

Table 4
Isoconversion parameters for PVA in 10% Ag–PVA nanocomposite

Time (min)	Conversion (%)								
	10	20	30	40	50	60	70	80	90
10	490.5	500.4	505.5	509.2	512.3	515.2	518.0	521.2	525.5
30	474.9	484.5	488.9	492.2	494.7	497.1	499.5	501.8	504.7
50	468.0	477.4	481.6	484.7	487.0	489.1	491.3	493.2	495.5
70	463.6	472.9	476.9	479.9	482.0	484.0	486.0	487.8	489.7
90	460.3	469.5	473.4	476.3	478.3	480.3	482.2	483.8	485.4
120	456.7	465.8	469.5	472.3	474.2	476.1	477.8	479.3	480.6

Also, it was possible to estimate the temperature of the degradation process for pure PVA and PVA in nanocomposite system, predicted by model-free data, providing an estimation of the time required for the degradation reaction, as summarized in Tables 1–4.

It was observed, for instance, that for pure PVA to achieve a 30% conversion it was necessary to subject it to a temperature of 468 °C for 90 min, whereas for the PVA with 0.5% of Ag nanoparticles to achieve the same degradation in the same period of time a temperature of 473 °C was necessary; with 2.5% of Ag nanoparticles a temperature of 476 °C was necessary, and for the PVA with 10% of Ag nanoparticles a temperature of 473 °C. Also it can be seen that for the PVA with 0.5% of Ag nanoparticles and for small conversions, acceleration of degradation occurred, indicating changes in degradation mechanism, but this should be studied further.

4. Conclusions

Dynamic thermal degradation of pure PVA and PVA in nanocomposite system with Ag nanoparticles obtained by gamma irradiation was carried out in the temperature range from 30 to 600 °C at heating rates of 5, 10 and 20 °C min^{-1}. In this temperature range the thermal degradation of pure PVA occurs through two degradation steps. The thermal degradation of the PVA in nanocomposite with Ag nanoparticles changes with the content of the nanofiller and for the higher content of Ag the second degradation step vanishes suggesting the degradation via competitive reactions. The addition of Ag nanoparticles increases the onset temperatures and the temperatures at the maximum rates of degradation in the first degradation step compared with pure PVA.

The model-free kinetics applied in this investigation has proven to be an evaluation tool in the study of the thermal degradation process of PVA with and without Ag nanofiller, even considering the small percentage added to the polymer. The thermogravimetric study provides an important link between the degradation temperatures and thermal profiles of both pure PVA and PVA loaded with Ag nanoparticles. The results of activation energy show that the PVA containing Ag nanoparticles has greater thermal stability than pure PVA.

Acknowledgement

This study was supported by the Serbian ministry of Science and Environmental Protection, Project No. 142066.

References

[1] K.L. Kelly, E. Coronado, L.L. Zhao, G.C. Schatz, J. Phys. Chem. B 107 (2003) 668.
[2] P. Mulvaney, Langmuir 12 (1996) 788.
[3] B. Karthikeyan, Physica B 364 (2005) 328.
[4] G.A. Gaddy, A.S. Korchev, J.L. McLain, B.L. Slaten, E.S. Steigerwalt, G. Mills, J. Phys. Chem. B 108 (2004) 14850.
[5] P.K. Khanna, N. Singh, S. Charan, V.V.V.S. Subbarao, R. Gokhale, U.P. Mulik, Mater. Chem. Phys. 93 (2005) 117.
[6] R. He, X. Qian, J. Yin, Z. Zhu, J. Mater. Chem. 12 (2002) 3783.
[7] F. Mafuné, J.Y. Kohno, Y. Takeda, T. Kondow, H. Sawabe, J. Phys. Chem. B 104 (2000) 9111.
[8] Y. Zhou, S.H. Yu, C.Y. Wang, X.G. Li, Y.R. Zhu, Z.Y. Chen, Adv. Mater. 11 (1999) 850.
[9] K.S. Morley, P.B. Webb, N.V. Tokareva, A.P. Krasnov, V.K. Popov, J. Zhang, C.J. Roberts, S.M. Howdle, Eur. Polym. J. 34 (2007) 307.
[10] J. Sloan, D.M. Wright, H.G. Woo, S. Bailey, G. Brown, A.P.E. York, K.S. Coleman, J.L. Hutchison, M.L.H. Green, Chem. Commun. 8 (1999) 699.
[11] A. Krklješ, J.M. Nedeljković, Z.M. Kačarević-Popović, Polym. Bull. 58 (2007) 271.
[12] A. Henglein, J. Phys. Chem. 97 (1993) 5457.
[13] J. Belloni, M. Mostafavi, H. Remita, J.L. Marignier, M.O. Delcourt, New J. Chem. 22 (1998) 1239.
[14] M.K. Temgire, S.S. Joshi, Radiat. Phys. Chem. 71 (2004) 1039.
[15] A.N. Krklješ, M.T. Marinović-Cincović, Z.M. Kačarević-Popović, J.M. Nedeljković, Eur. Polym. J. 43 (6) (2007) 2171.
[16] H. Remita, I. Lampre, M. Mostafavi, E. Balanzat, S. Bouffard, Radiat. Phys. Chem. 72 (2005) 575.
[17] J. Kuljanin, M.I. Čomor, V. Djoković, J.M. Nedeljković, Mater. Chem. Phys. 95 (2006) 67.
[18] M. Marinovic-Cincovic, Z. Saponjic, V. Djokovic, S. Milonjic, J. Nedeljkovic, Polym. Degrad. Stab. 91 (2006) 313.
[19] M. Marinovic-Cincovic, M.C. Popovic, M.M. Novakovic, J.M. Nedeljkovic, Polym. Degrad. Stab. 92 (2007) 70.
[20] J. Kuljanin, M. Marinovic-Cincovic, S. Zec, M.I. Comor, J.M. Nedeljkovic, J. Mater. Sci. Lett. 22 (2003) 235.
[21] D. Sajinovic, Z. Saponjic, N. Cvjeticanin, M. Marinovic-Cincovic, J. Nedeljkovic, Chem. Phys. Lett. 329 (2000) 168.
[22] Z. Peng, L.X. Kong, S. Li, P. Spiridonov, J. Nanosci. Nanotechnol. 6 (2006) 3934.
[23] J. Lee, Y. Liao, R. Nagahata, Sh. Horiuchi, Polymer 47 (2006) 7970.
[24] E. Tadd, A. Zeno, M. Zubris, N. Dan, R. Tannenbaum, Macromolecules 36 (2003) 6497.
[25] Y. Li, K.G. Neoh, E.T. Kang, Polymer 45 (2004) 8779.
[26] S. Vyazovkin, N. Sbirrayyuoli, Macromol. Rapid Commun. 27 (2006) 1515.
[27] H. Polli, L.A.M. Pontes, M.J.B. Souza, V.J. Fernandes, A.S. Araujo, J. Therm. Anal. Calorim. 86 (2006) 469.
[28] O. Levenspil, Chemical Reaction Engineering, 2nd ed., John Wiely & Sons, New York, 1972 (Chapt. 8).
[29] J.W. Gilman, D.L. Vanderhart, T. Kashiwagi, ACS Symposium Series 599, Washington, DC, 1994, p. 161.
[30] B. Wang, M. Kodama, S. Mukataka, E. Kokofuta, Polym. Gels Netw. 6 (1998) 71.
[31] A. Chapiro, High Polymers. Volume XV: Radiation Chemistry of Polymeric Systems, John Wiley & Sons Inc., 1962, p. 588.
[32] A.N. Krklješ, Z.M. Kačarević-Popović, J.M. Nedeljković, Nucl. Instr. Meth. Phys. Res. B, submitted for publication.
[33] Z.H. Mibhele, M.G. Salemane, C.G.C.E. van Sittert, J.M. Nedeljkovic, V. Djokovic, A.S. Luyt, Chem. Mater. 15 (2003) 5019.
[34] S. Vyazovkin, Int. J. Chem. Kinet. 28 (1996) 95.
[35] S. Vyazovkin, Ch. Wight, Thermochim. Acta 340/341 (1999) 53.
[36] H. Polli, L.A.M. Pontes, A.S. Araujo, J. Therm. Anal. Calorim. 79 (2005) 383.